

## Bis-isonicotinoyl linkers containing polyaromatic scaffolds: synthesis, structure and spectroscopic properties.

Andrea Delledonne,<sup>a</sup> Martina Orlandini,<sup>a</sup> Paolo P. Mazzeo,<sup>a,b</sup> Cristina Sissa,<sup>a</sup> Alessia Bacchi,<sup>a,b</sup> Francesca Terenziani<sup>\*,a</sup> and Paolo Pelagatti<sup>\*,a,c</sup>

<sup>a</sup> Department of Chemical Sciences, Life Science and Environmental Sustainability, University of Parma, Parco Area delle Scienze 17/A, 43124 Parma, Italy

<sup>b</sup> Biopharmanet-TEC, University of Parma, Parco Area delle Scienze 27/A, 43124 Parma, Italy

<sup>c</sup> CIRCC, Interuniversity Consortium of Chemical Reactivity and Catalysis, via Celso Ulpiani 27, 70126 Bari, Italy

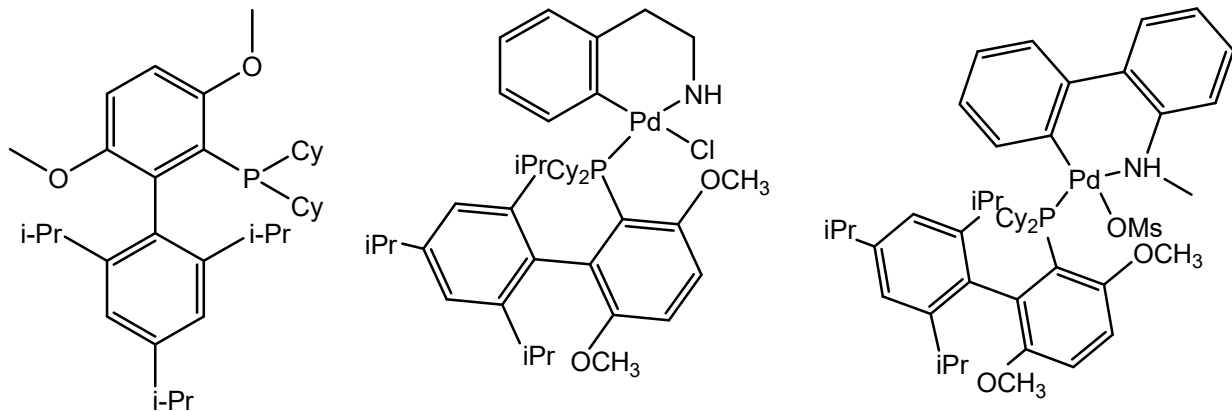
## Supporting information

pp 19

<b>General</b> .....	1
<b>FT-IR spectroscopy</b> .....	2
<b><sup>1</sup>HNMR spectroscopy</b> .....	5
<b>Mass spectra</b> .....	8
<b>Crystallography</b> .....	11
<b>Spectroscopic characterization</b> .....	14
<b>TDDFT calculations</b> .....	15

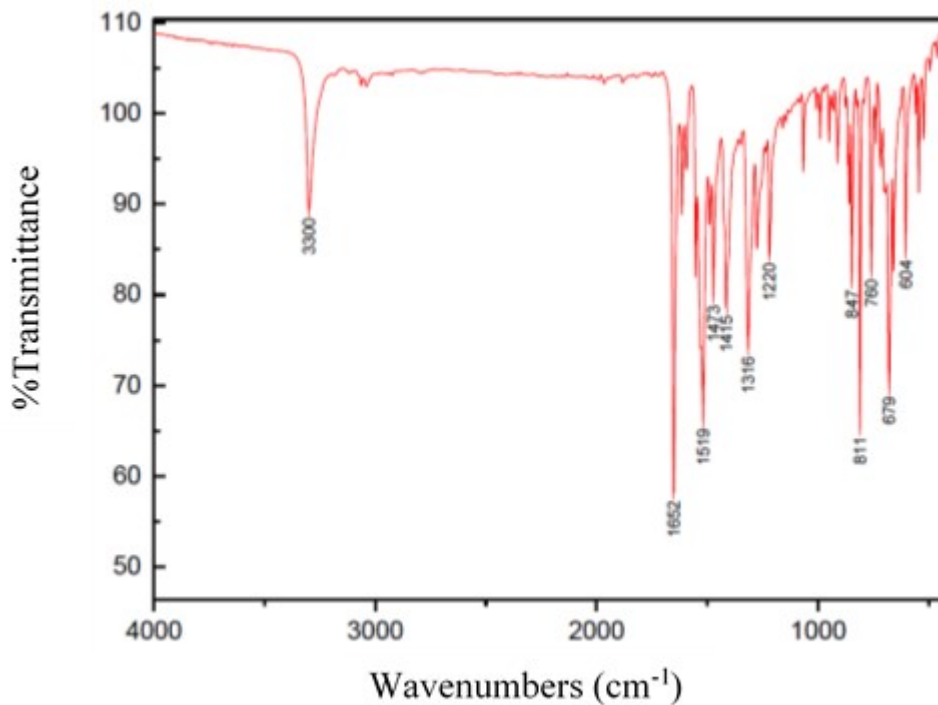
## General

### Structure of catalysts employed

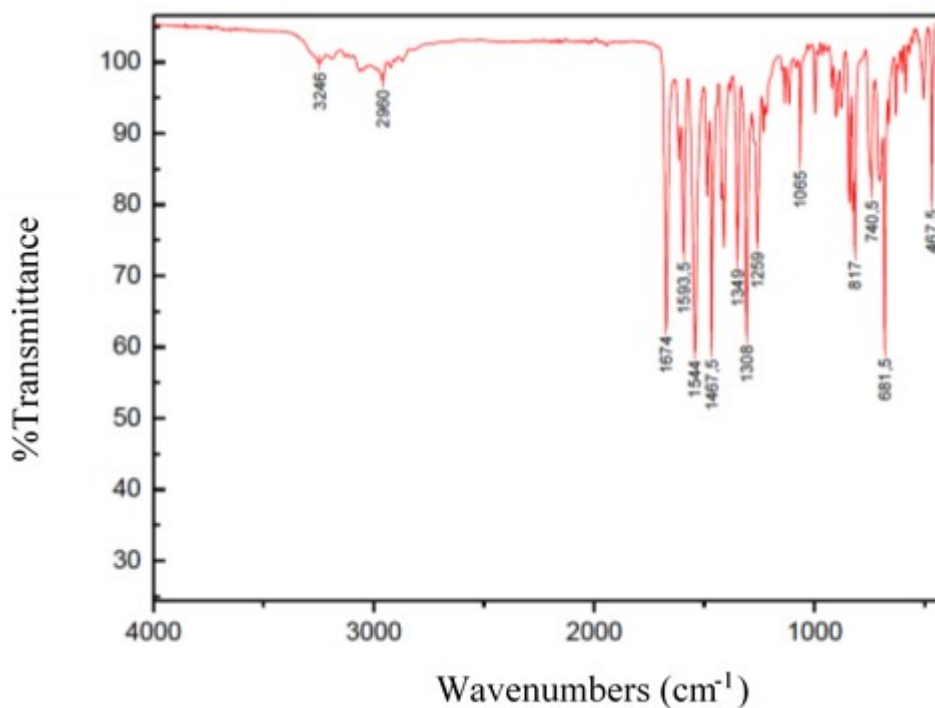


**Scheme S1** Structures of BrettPhos, PdG1 (methyl-t-butyl ether molecule is omitted) and PdG4

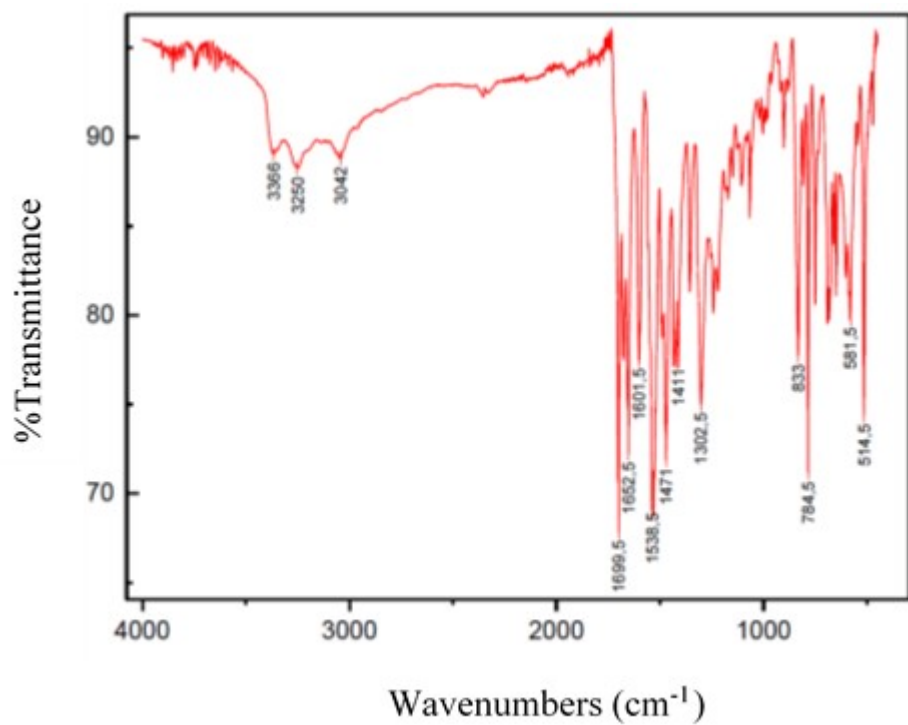
## FT-IR spectroscopy



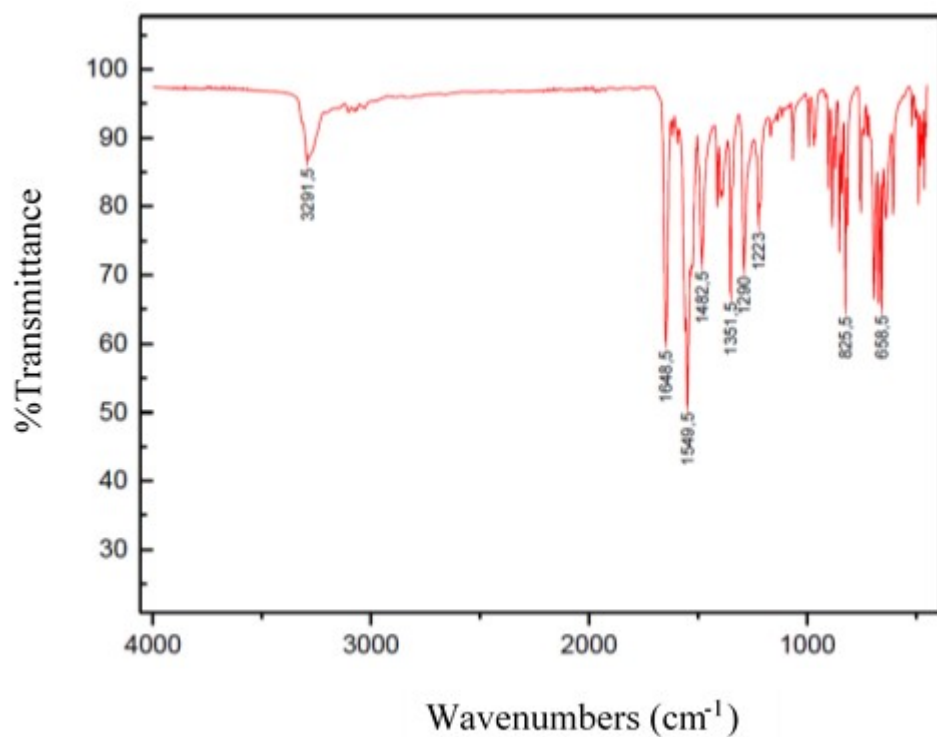
**Figure S1** FT-IR spectrum of **1**



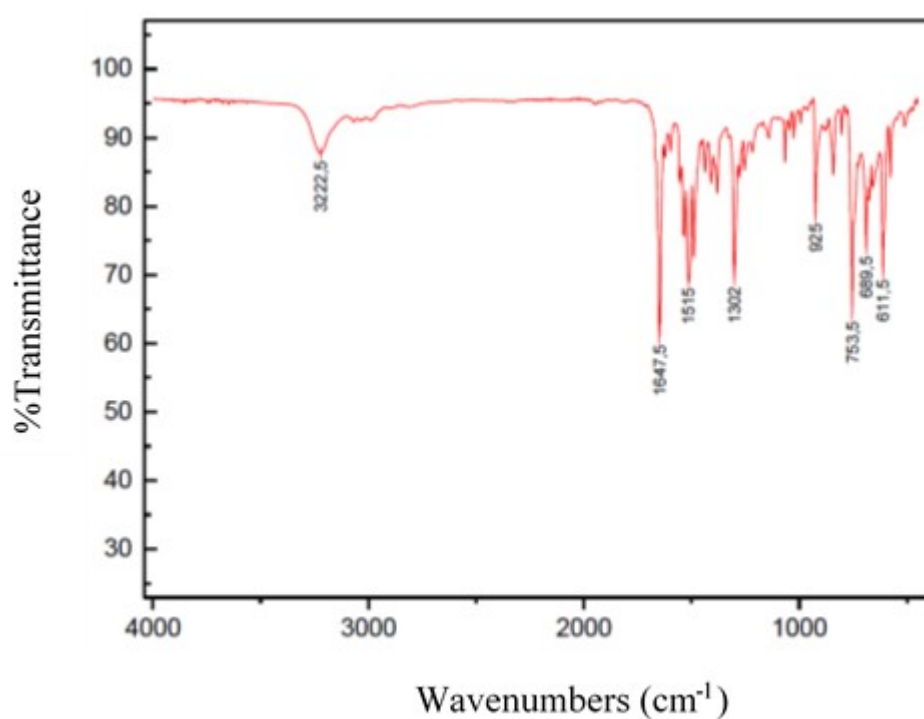
**Figure S2** FT-IR spectrum of **2**



**Figure S3** FT-IR spectrum of **3**

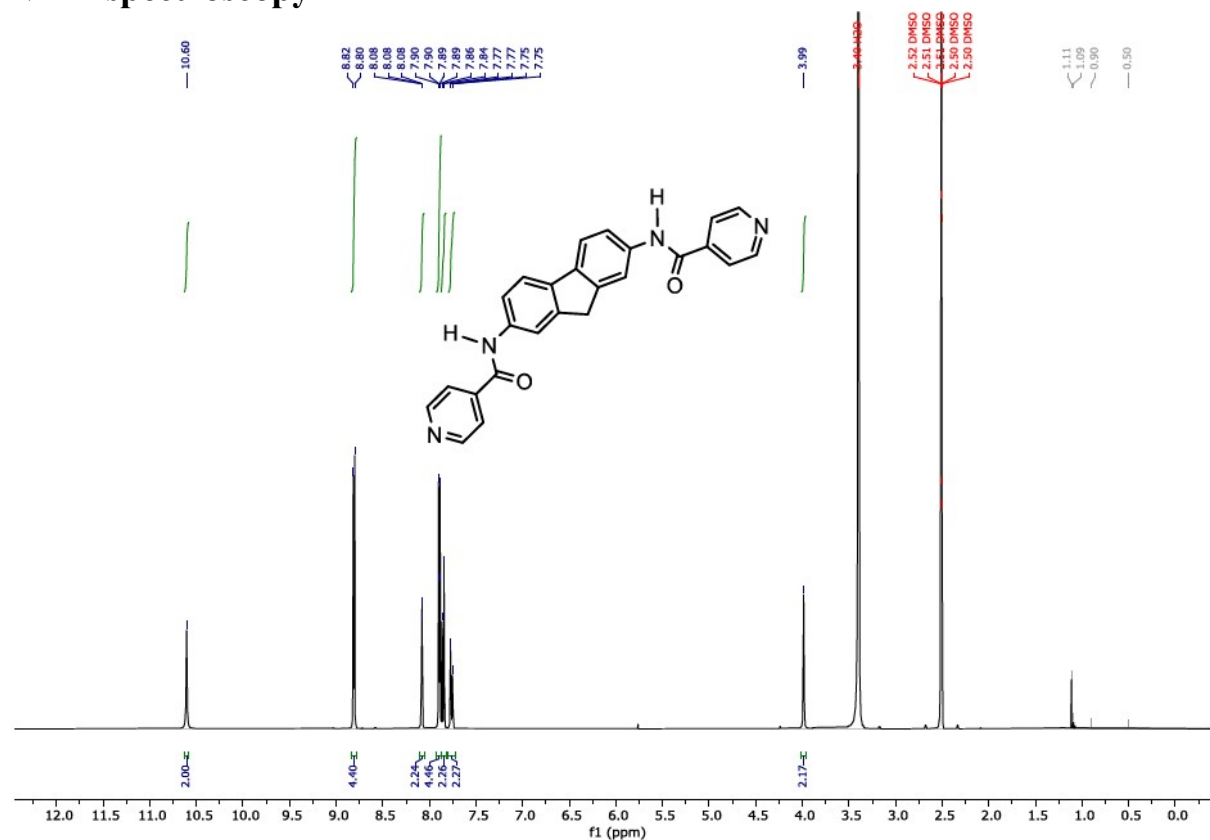


**Figure S4** FT-IR spectrum of **4**

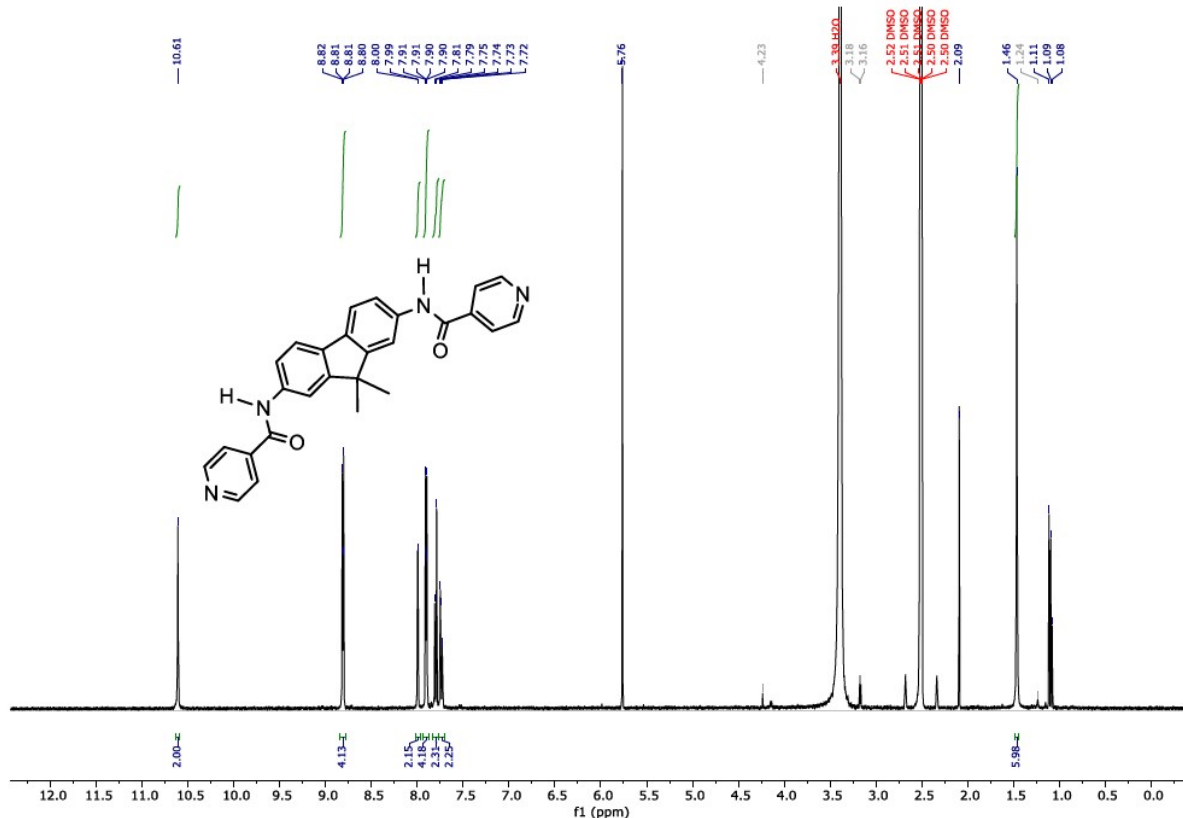


**Figure S5** FT-IR spectrum of **5**

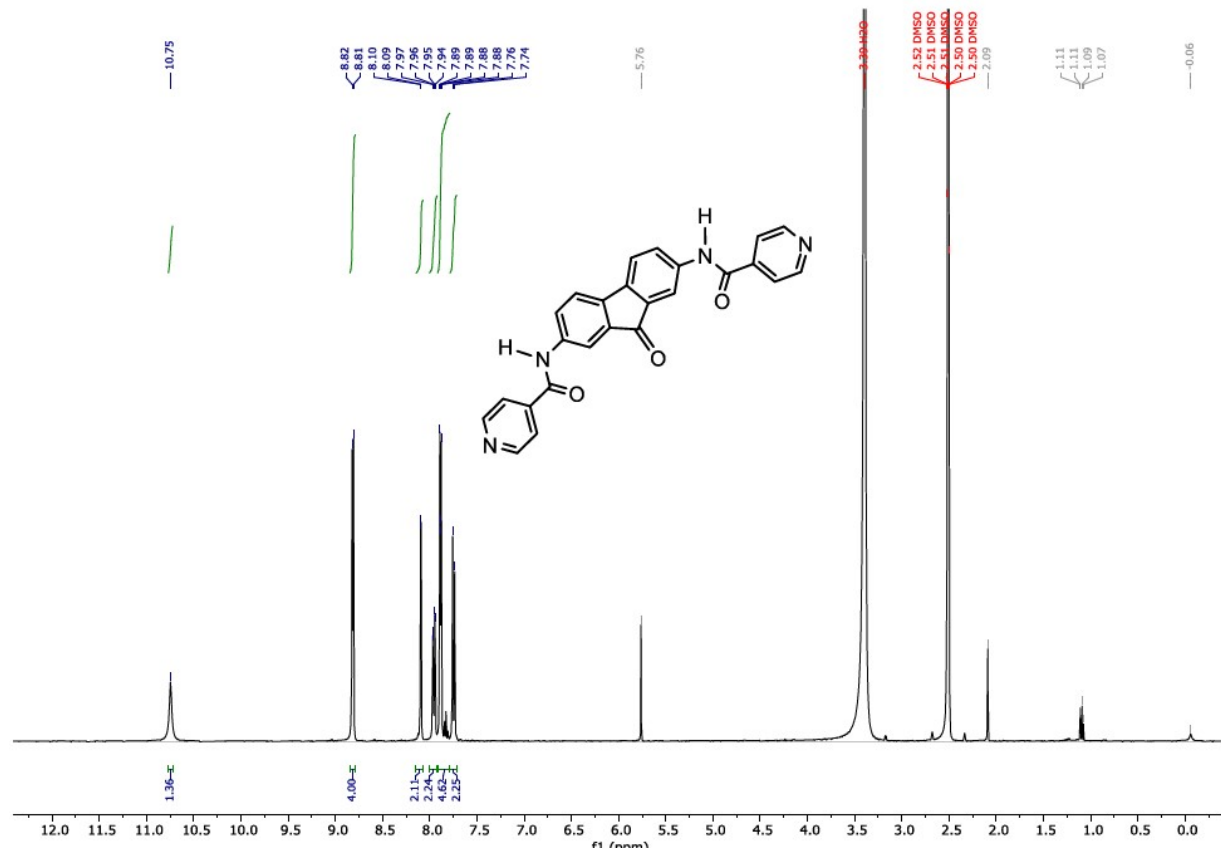
## <sup>1</sup>H NMR spectroscopy



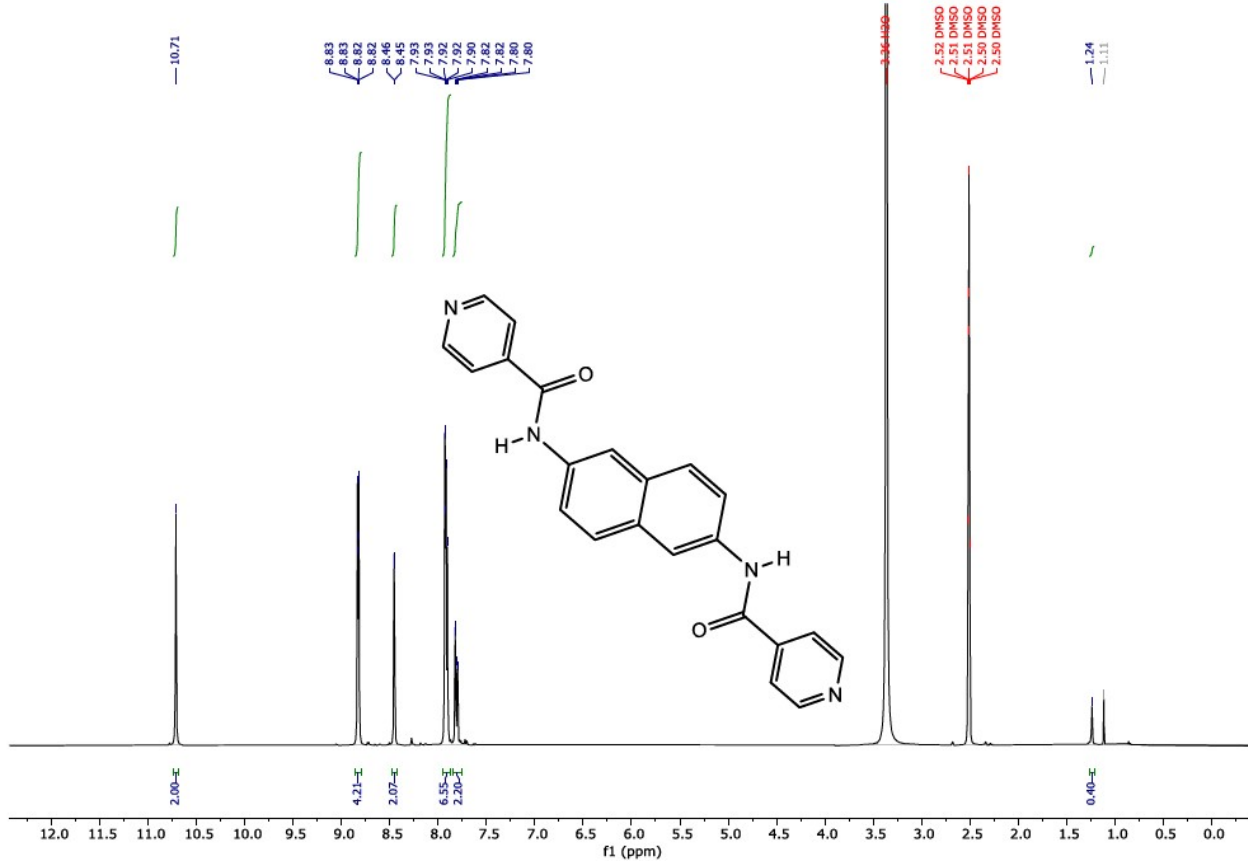
**Figure S6** <sup>1</sup>H NMR spectrum of **1** (DMSO-d<sub>6</sub>, 400 MHz, 25°C)



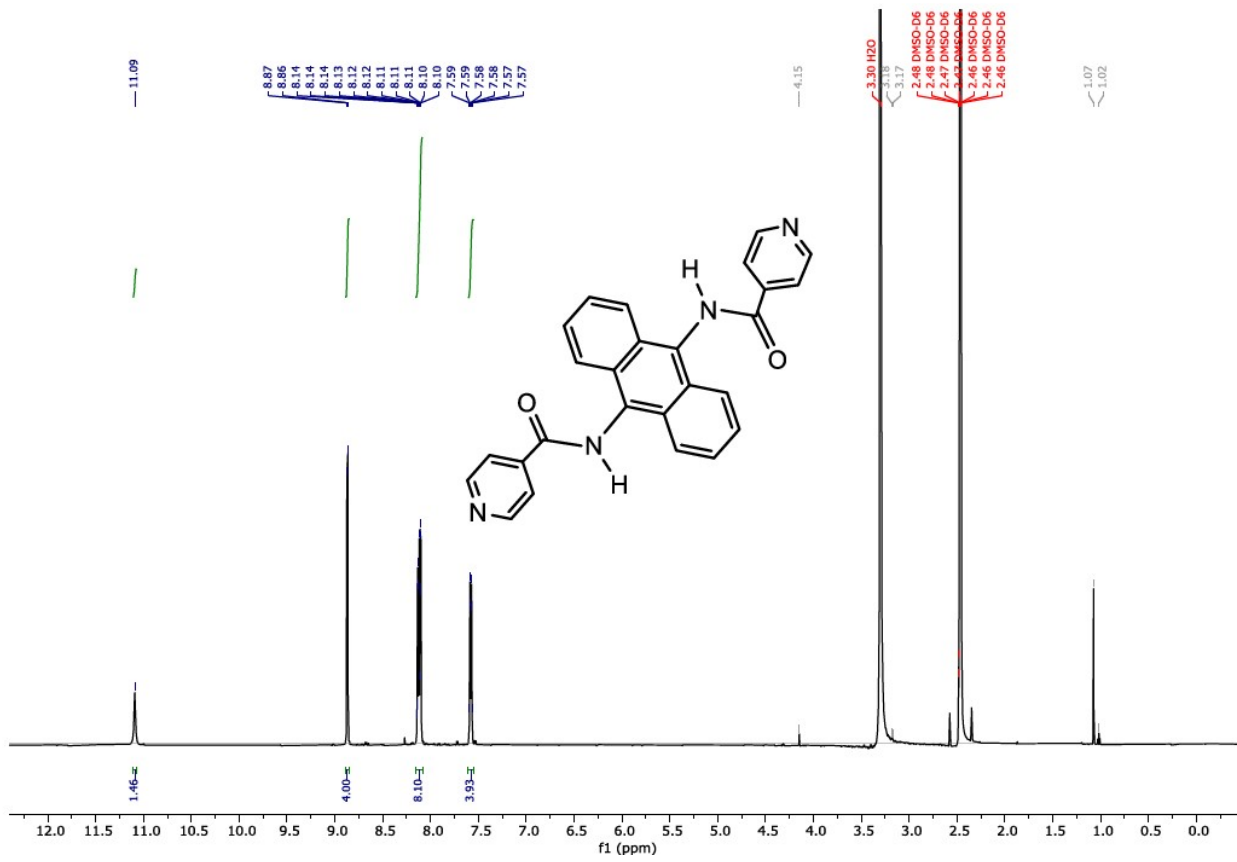
**Figure S7** <sup>1</sup>H NMR spectrum of **2** (DMSO-d<sub>6</sub>, 400 MHz, 25°C)



**Figure S8**  $^1\text{H}$  NMR spectrum of **3** (DMSO- $d_6$ , 400 MHz, 25°C)

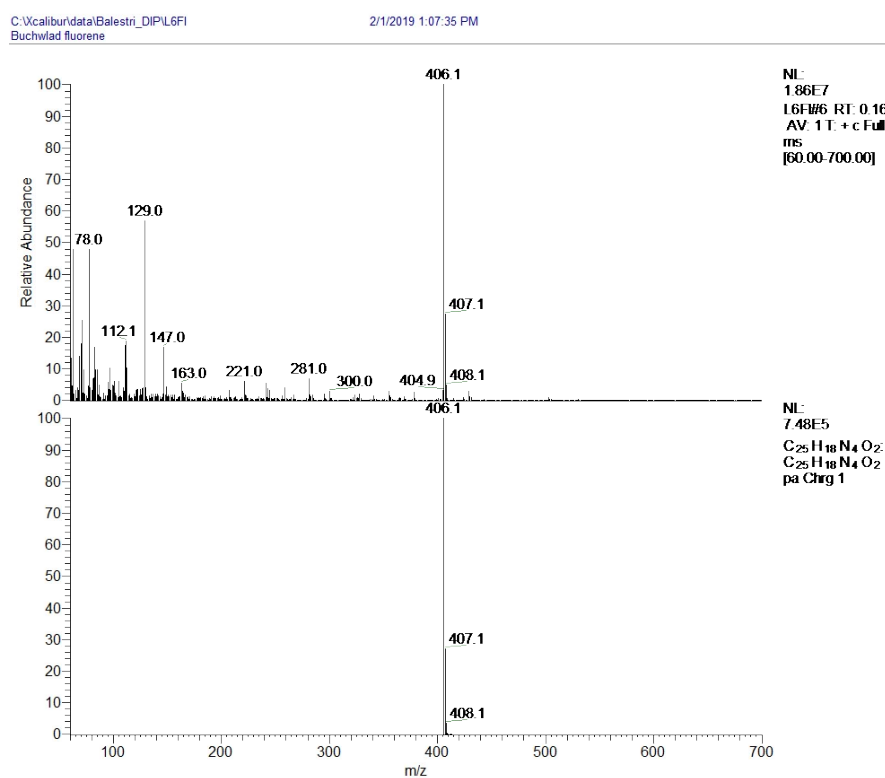


**Figure S9**  $^1\text{H}$  NMR spectrum of **4** (DMSO- $d_6$ , 400 MHz, 25°C)

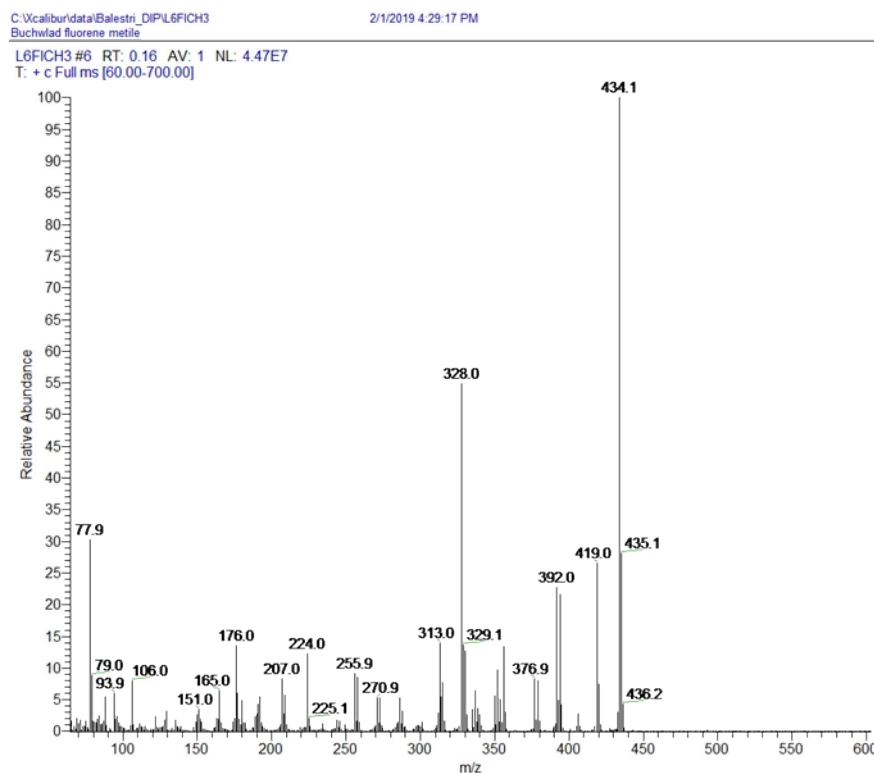


**Figure S10**  $^1\text{H}$  NMR spectrum of **5** (DMSO- $\text{d}_6$ , 400 MHz, 25°C)

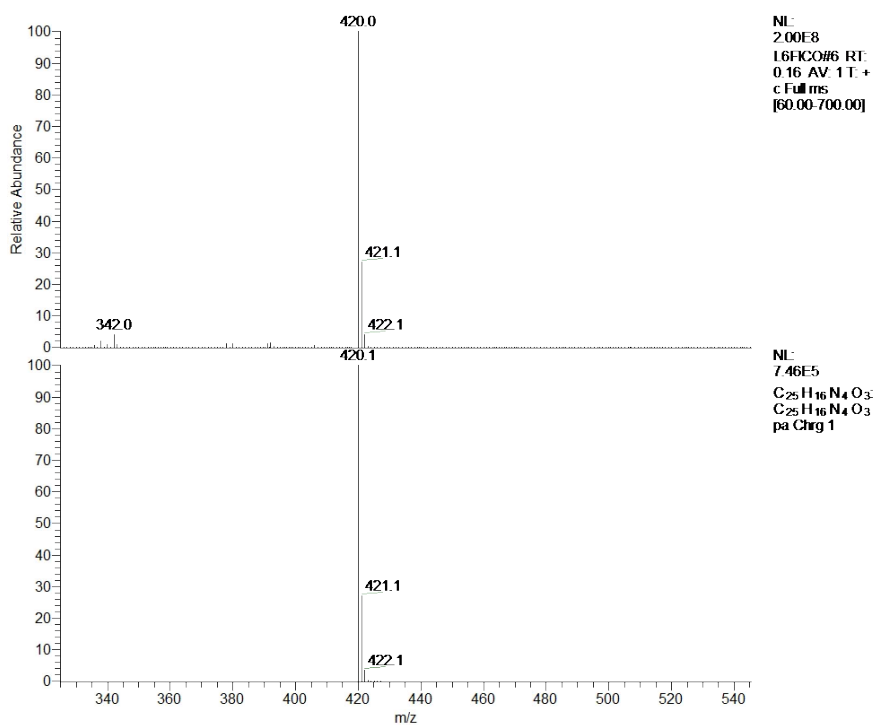
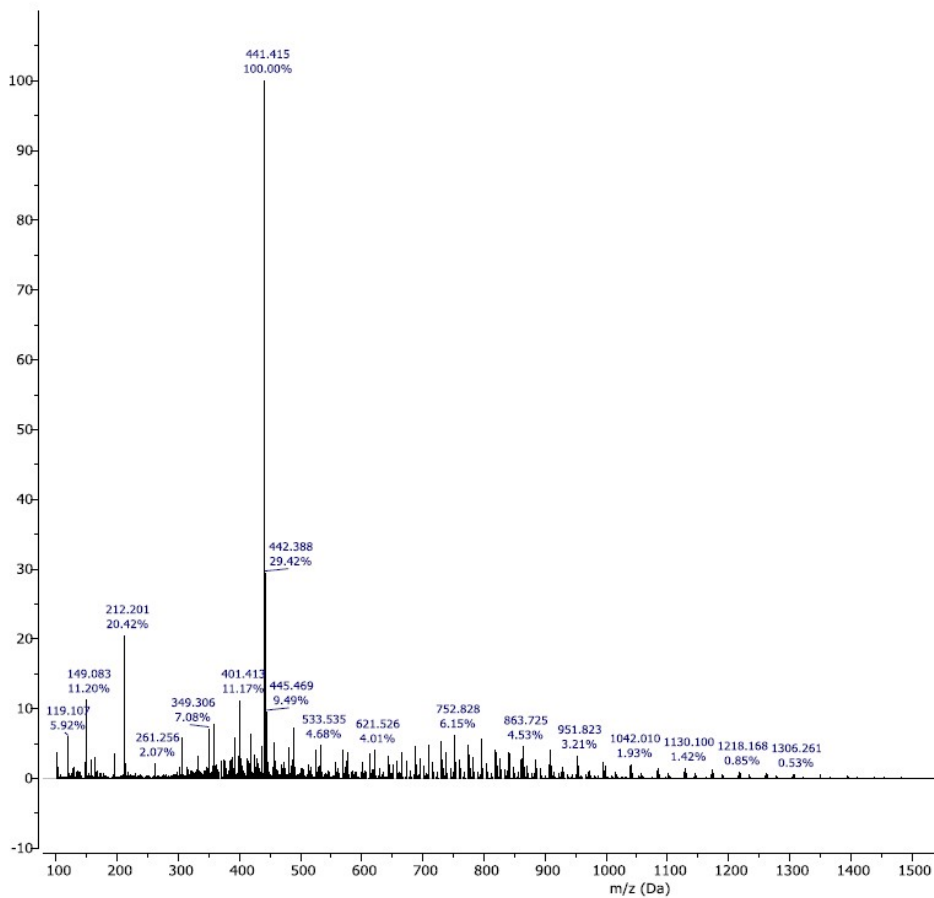
## Mass spectra



**Figure S11** EI-MS(+) of spectrum of 1



**Figure S12** EI-MS(+) spectrum of 2

**Figure S13** EI-MS(+) spectrum of **3****Figure S14** ESI-MS(+) spectrum of **5** (methanol, 50 V)

## Crystallography

**Table S1.** Crystallographic data and structure refinement for **1–5**. Crystallographic data have been deposited with the CCDC 2098423–2098427 refcodes.

Identification code	1	2	3	4	5
Empirical formula	C <sub>25</sub> H <sub>18</sub> N <sub>4</sub> O <sub>2</sub>	C <sub>27</sub> H <sub>22</sub> N <sub>4</sub> O <sub>2</sub>	C <sub>25</sub> H <sub>16</sub> N <sub>4</sub> O <sub>3</sub> ·2H <sub>2</sub> O	C <sub>11</sub> H <sub>8</sub> N <sub>2</sub> O·(C <sub>2</sub> H <sub>6</sub> SO)	C <sub>13</sub> H <sub>9</sub> N <sub>2</sub> O·(C <sub>2</sub> H <sub>6</sub> SO)
Formula weight	406.43	434.48	456.45	262.32	287.35
Temperature/K	200.0	200.0	200.0	297.0	297.0
Crystal system	monoclinic	triclinic	monoclinic	triclinic	triclinic
Space group	P2 <sub>1</sub> /n	P-1	C2/c	P-1	P-1
a/Å	7.7678(2)	9.1477(9)	13.5492(10)	7.6003(5)	9.1303(5)
b/Å	5.82960(10)	10.3739(8)	7.4023(5)	9.7756(7)	9.5438(5)
c/Å	42.6250(9)	25.486(3)	21.4841(16)	9.7883(7)	18.2326(9)
$\alpha/^\circ$	90	89.281(5)	90	96.092(2)	86.920(2)
$\beta/^\circ$	91.468(2)	79.975(6)	100.382(2)	103.963(2)	78.265(2)
$\gamma/^\circ$	90	67.010(5)	90	111.340(3)	66.827(2)
Volume/Å <sup>3</sup>	1929.56(7)	2188.4(4)	2119.5(3)	642.06(8)	1429.43(13)
Z	4	4	4	2	4
$\rho_{\text{calc}}/\text{g cm}^{-3}$	1.399	1.319	1.430	1.357	1.335
$\mu/\text{mm}^{-1}$	0.738	0.684	0.102	0.247	0.229
F(000)	848.0	912.0	952.0	276.0	604.0
0.08	0.07	0.08	0.08	0.09	
Crystal size/mm <sup>3</sup>	0.08	0.06	0.06	0.06	0.07
	0.06	0.06	0.04	0.04	0.06
Radiation	CuK $\alpha$	CuK $\alpha$	MoK $\alpha$	MoK $\alpha$	MoK $\alpha$
	( $\lambda = 1.54178$ )	( $\lambda = 1.54178$ )	( $\lambda = 0.71073$ )	( $\lambda = 0.71073$ )	( $\lambda = 0.71073$ )
2 $\Theta$ range for data collection/°	8.3 to 148.87	3.526 to 149.91	3.854 to 53.096	4.39 to 52.934	4.644 to 52.94
	-9 ≤ h ≤ 9	-10 ≤ h ≤ 11	-16 ≤ h ≤ 16	-9 ≤ h ≤ 9	-10 ≤ h ≤ 11
Index ranges	-7 ≤ k ≤ 7	-9 ≤ k ≤ 12	-9 ≤ k ≤ 8	-12 ≤ k ≤ 9	-11 ≤ k ≤ 11
	-53 ≤ l ≤ 53	-31 ≤ l ≤ 30	-26 ≤ l ≤ 26	-12 ≤ l ≤ 12	-20 ≤ l ≤ 22
Reflections collected	34359	24434	11535	6838	15101
	3947	7702	2197	2640	5819
Independent reflections	R <sub>int</sub> = 0.1363	R <sub>int</sub> = 0.1801	R <sub>int</sub> = 0.0590	R <sub>int</sub> = 0.0378	R <sub>int</sub> = 0.0357
	R <sub>sigma</sub> = 0.0628	R <sub>sigma</sub> = 0.1808	R <sub>sigma</sub> = 0.0482	R <sub>sigma</sub> = 0.0500	R <sub>sigma</sub> = 0.0459
Data/restraints/parameters	3947/0/280	7702/0/635	2197/0/158	2640/0/165	5819/0/365
Goodness-of-fit on F <sup>2</sup>	1.011	0.938	1.124	1.030	0.733
Final R indexes	R <sub>1</sub> = 0.0585	R <sub>1</sub> = 0.0931	R <sub>1</sub> = 0.0733	R <sub>1</sub> = 0.0447	R <sub>1</sub> = 0.0545
[I >= 2σ (I)]	wR <sub>2</sub> = 0.1410	wR <sub>2</sub> = 0.2102	wR <sub>2</sub> = 0.1461	wR <sub>2</sub> = 0.0947	wR <sub>2</sub> = 0.1699
Final R indexes	R <sub>1</sub> = 0.1052	R <sub>1</sub> = 0.2545	R <sub>1</sub> = 0.1008	R <sub>1</sub> = 0.0679	R <sub>1</sub> = 0.0699
[all data]	wR <sub>2</sub> = 0.1713	wR <sub>2</sub> = 0.2999	wR <sub>2</sub> = 0.1582	wR <sub>2</sub> = 0.1073	wR <sub>2</sub> = 0.1935
Largest diff. peak/hole / e Å <sup>-3</sup>	0.21/-0.33	0.28/-0.33	0.39/-0.26	0.19/-0.24	1.10/-0.46

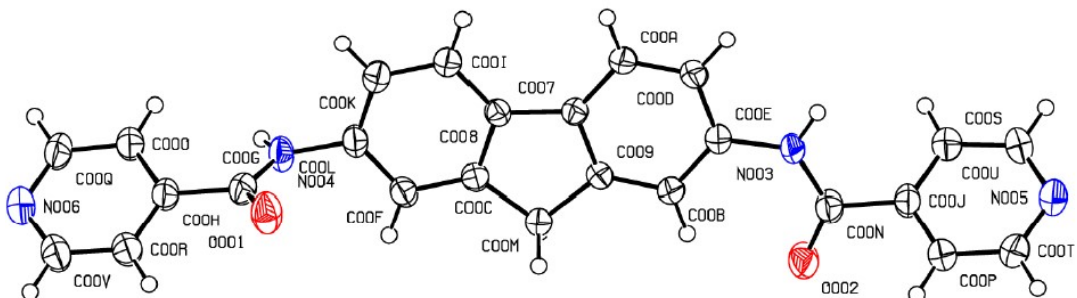


**Figure S15:** ORTEP drawing of **1**. All non-hydrogen atoms are shown as ellipsoids at the 50% probability level. H atoms (isotropically refined) are reported in ball-and-stick style for the sake of clarity.

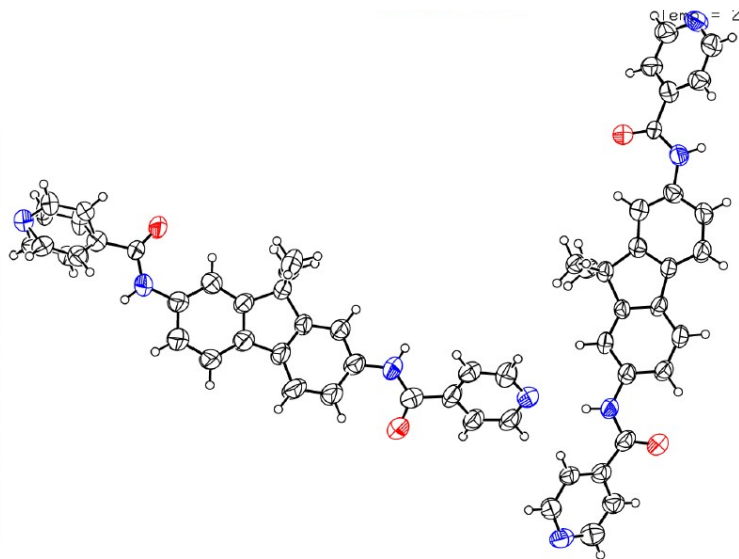


**Figure S16:** ORTEP drawing of **2**. All non-hydrogen atoms are shown as ellipsoids at the 50% probability level. H atoms (isotropically refined) are reported in ball-and-stick style and atom labels are omitted for the sake of clarity.

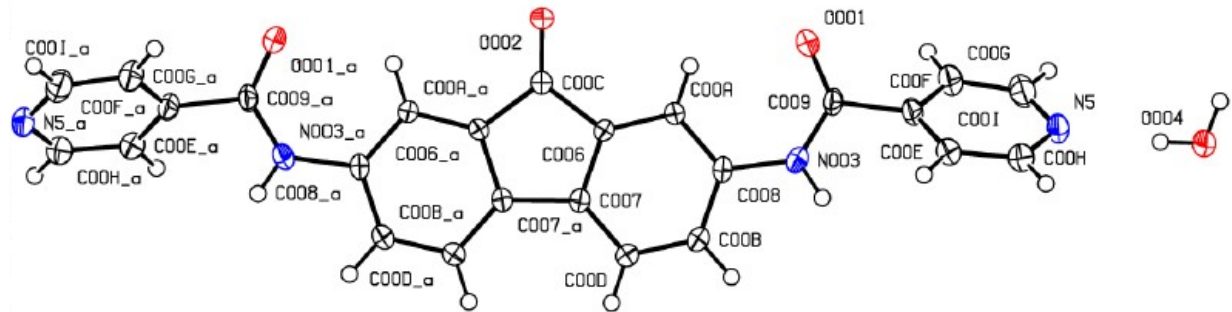


**Figure S18:** ORTEP drawing of **3**. All non-hydrogen atoms are shown as ellipsoids at the 50% probability level. H atoms (isotropically refined) are reported in ball-and-stick style for the sake of clarity.

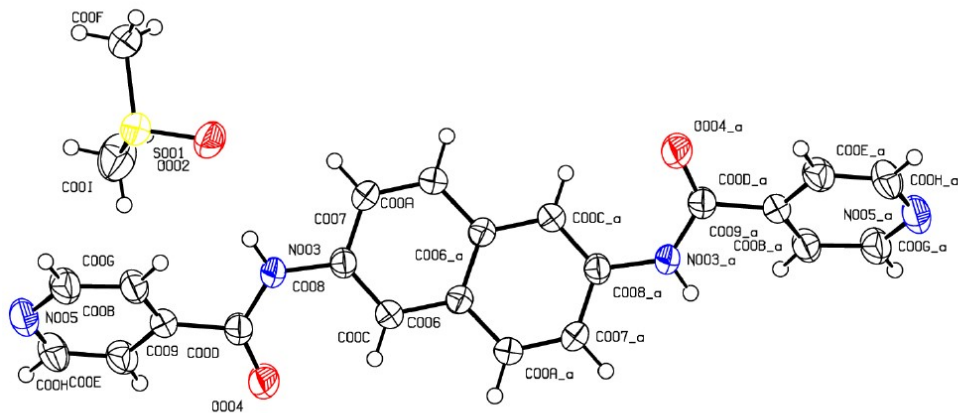


**Figure S19:** ORTEP drawing of **4**. All non-hydrogen atoms are shown as ellipsoids at the 50% probability level. H atoms (isotropically refined) are reported in ball-and-stick style for the sake of clarity.

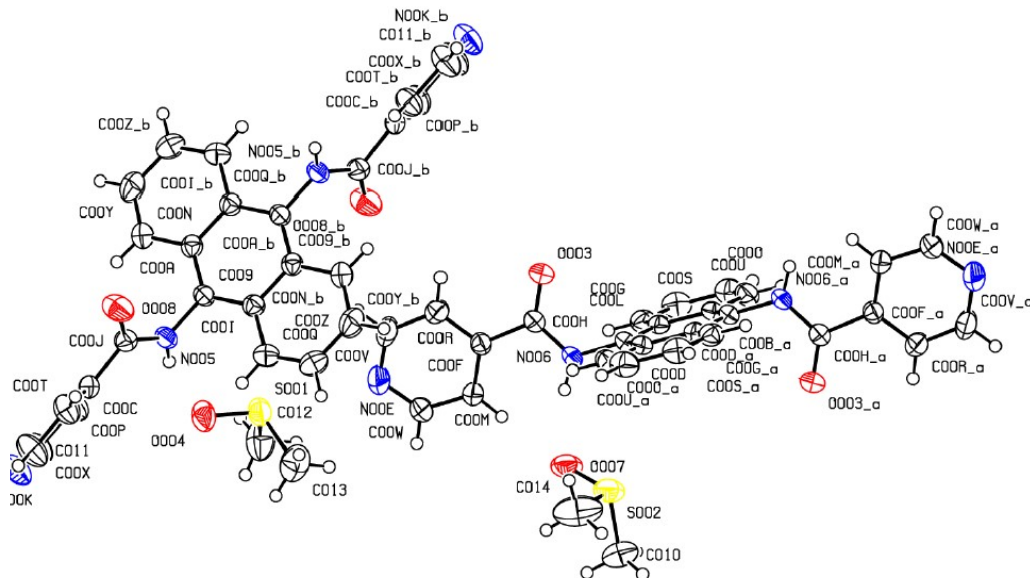


**Figure S20:** ORTEP drawing of **5**. All non-hydrogen atoms are shown as ellipsoids at the 50% probability level. H atoms (isotropically refined) are reported in ball-and-stick style for the sake of clarity.

## Spectroscopic characterization

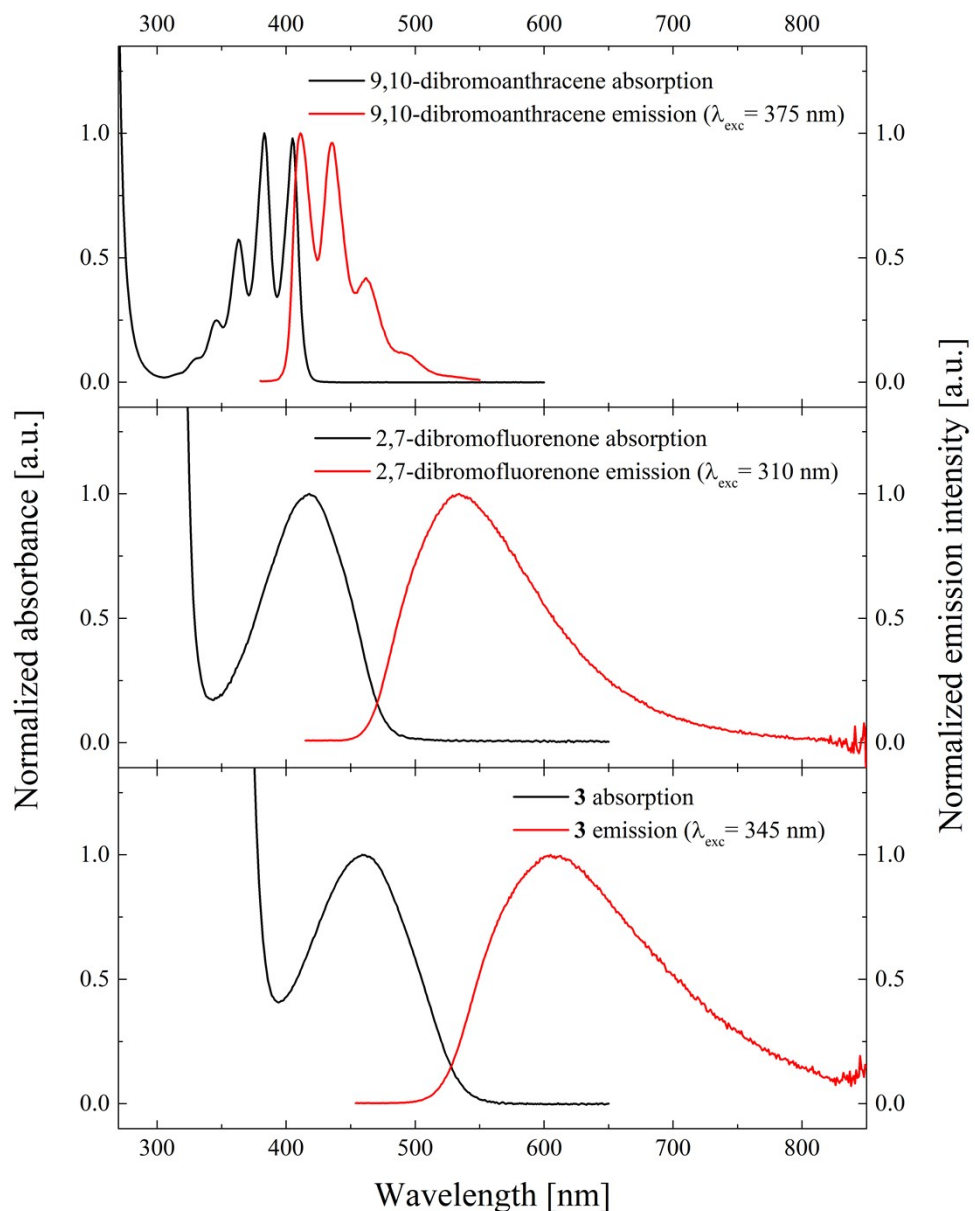


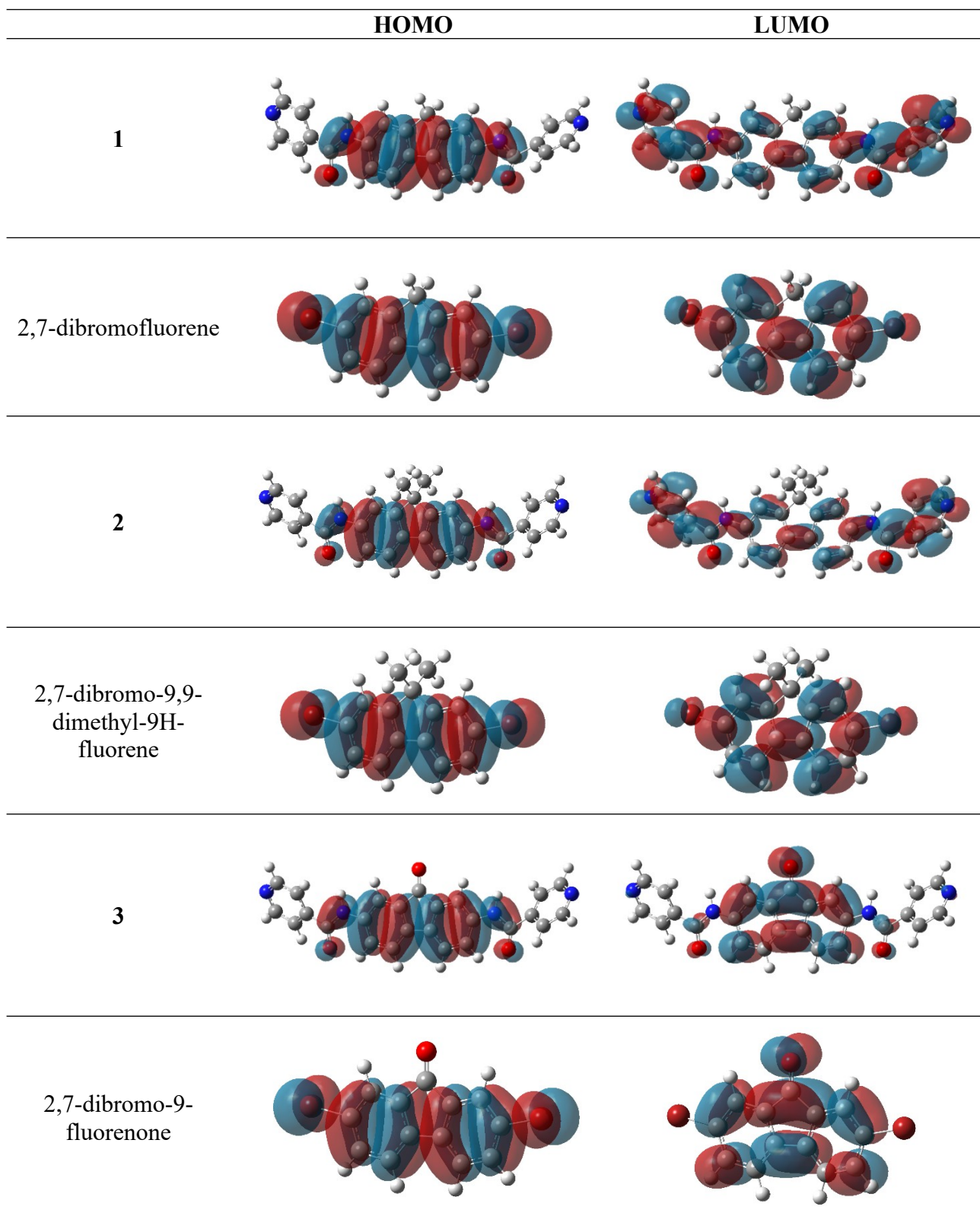
**Figure S21.** Absorption and emission spectra of linker **3**, 2,7-dibromofluorenone and 1,9-dibromoanthracene in DMF. The corresponding excitation and emission wavelengths are reported in the legend. Fluorescence quantum yield of **3** is <0.01 (fluorescein in NaOH 0.1M  $\phi=0.9$ )

**Table S2.** Absorption properties in DMF of ligands **1-6**.

Ligand	$\lambda_{\text{max}}^{\text{abs}}$ [nm]	Molar extinction coefficient [ $M^{-1}cm^{-1}$ ]
<b>1</b>	338	$4.80 \times 10^4$
<b>2</b>	340	$4.50 \times 10^4$
<b>3</b>	344, 459	$3.10 \times 10^4, 0.158 \times 10^4$
<b>4</b>	330	$2.13 \times 10^4$
<b>5</b>	375	$0.979 \times 10^4$
<b>6</b>	322	$3.31 \times 10^4$

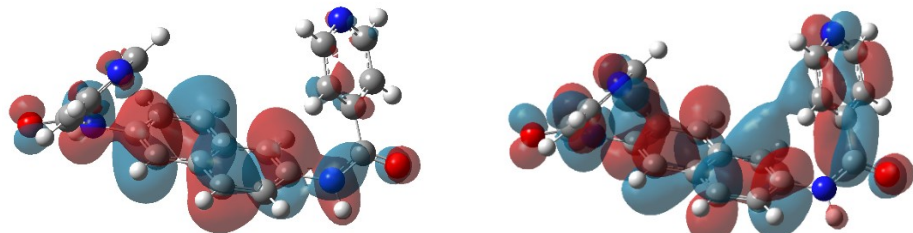
## TDDFT calculations

**Table S3.** HOMO/LUMO orbitals of linkers **1-6** and dibromo precursors.

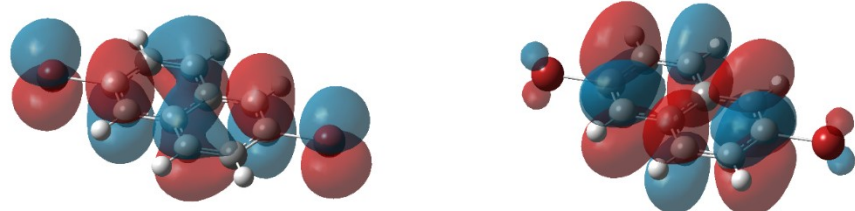


---

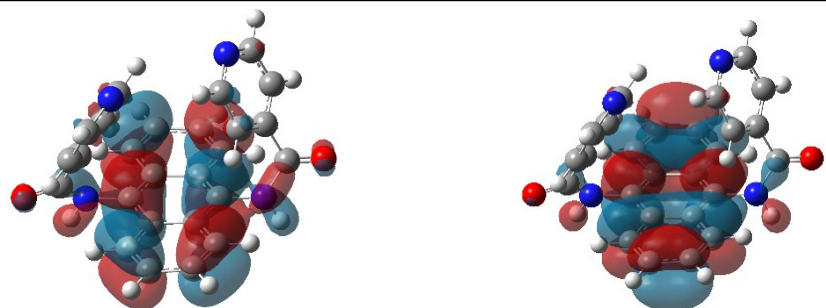
4



2,6-  
dibromonaphthalene



5



9,10-  
dibromoanthracene



6



4,4'-  
dibromobiphenylene



In order to inquire if multiple configurations are accessible at room temperature, a relaxed scan on the ground state potential energy surface of linker **6** has been performed, scanning over the two amide bonds dihedral angles using M062X as functional and 6-31G(d,p) as basis set.

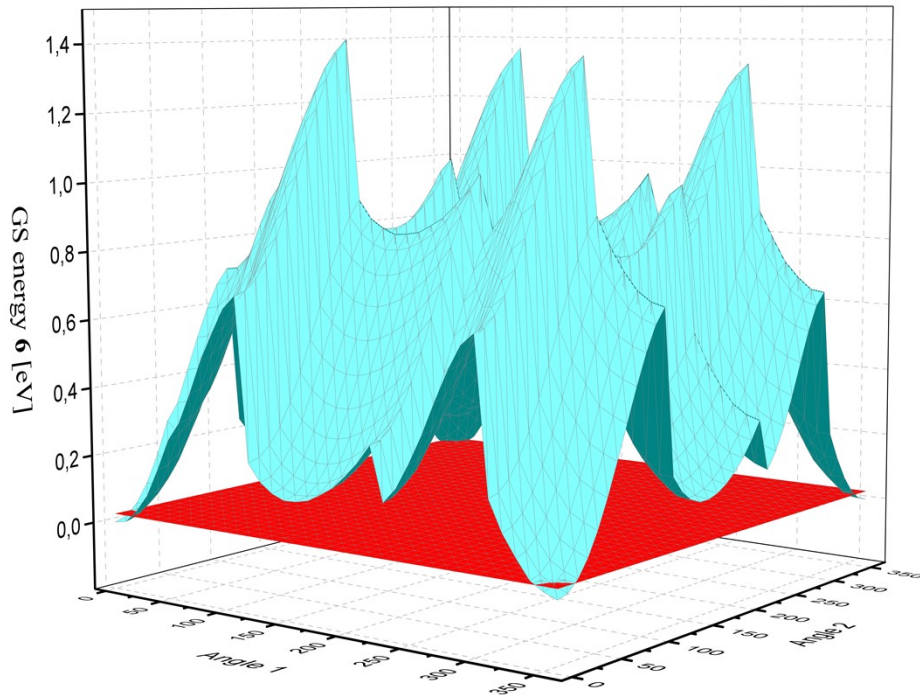


**Figure S22.** Ground state energy of linker **6** as a function of the two amide bonds dihedral angles. The red plane denotes the thermal energy at room temperature (0.025 eV).

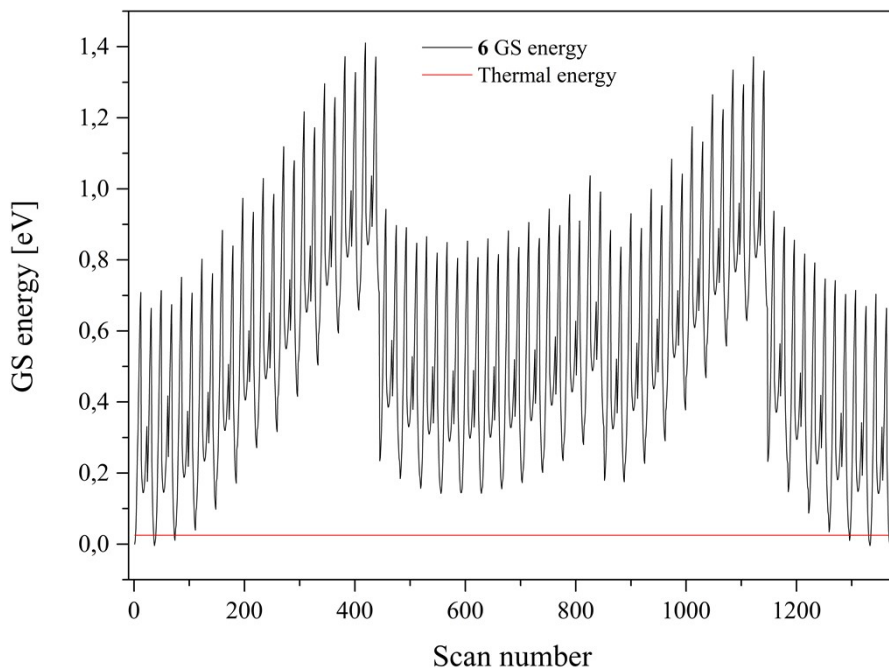


**Figure S23.** Ground state energy of linker **6** as a function of the scan number. In correspondence of each scan step, one of the two angles has been increased by 10 degrees, in order to make a complete rotation for both.

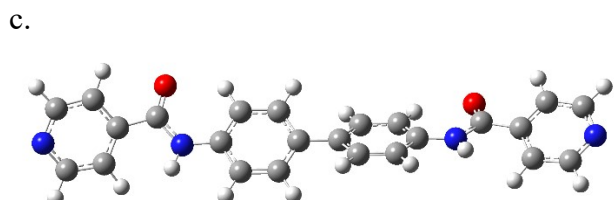
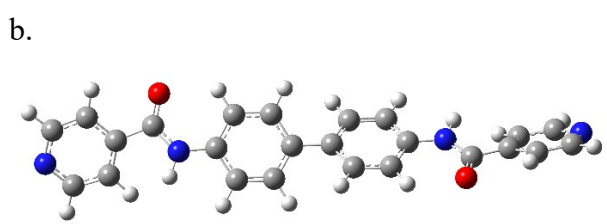
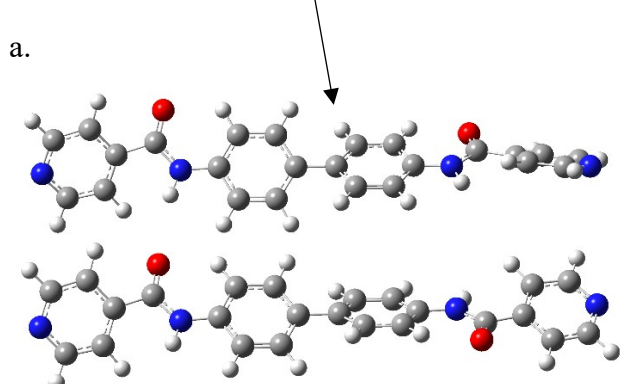
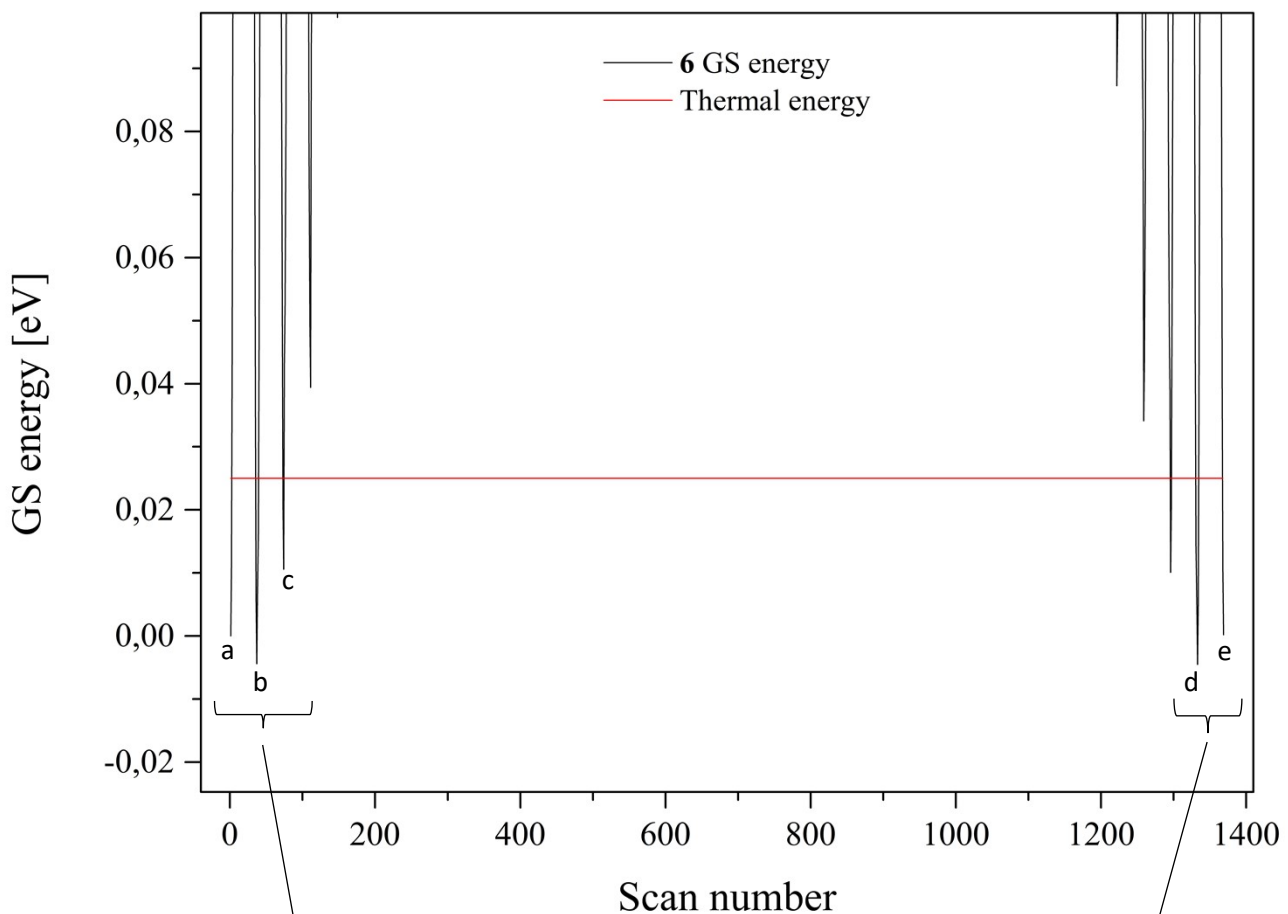


**Figure S24.** Above: enlargement of Figure S23; Below: linker **6** conformations characterized by lower energy than the thermal energy at room temperature.

**Table S4.** TDDFT results for ligand 4 in gas phase. The results for the first and second excited states are reported.

<i>Excited state</i>	<i>Transition energy [eV]</i>	<i>Oscillator strength</i>	<i>Main orbital contributions</i>	
1	4.24	0.03	HOMO → LUMO	(0.44)
			HOMO → LUMO+1	(-0.44)
2	4.41	0.16	HOMO → LUMO	(0.47)
			HOMO → LUMO+1	(0.33)